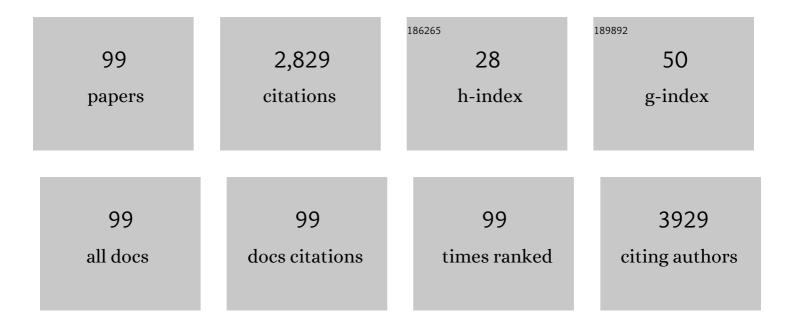
Massimo Catalano

List of Publications by Year in descending order

Source: https://exaly.com/author-pdf/2020846/publications.pdf Version: 2024-02-01



#	Article	IF	CITATIONS
1	Room Temperature Lasing at Blue Wavelengths in Gallium Nitride Microcavities. Science, 1999, 285, 1905-1906.	12.6	237
2	Ru Nanoframes with an fcc Structure and Enhanced Catalytic Properties. Nano Letters, 2016, 16, 2812-2817.	9.1	187
3	Synthesis and Characterization of CdS Nanoclusters in a Quaternary Microemulsion:  the Role of the Cosurfactant. Journal of Physical Chemistry B, 2000, 104, 8391-8397.	2.6	173
4	Silver nanocrystals in silica by sol-gel processing. Journal of Non-Crystalline Solids, 1996, 194, 225-234.	3.1	128
5	Formation of copper and silver nanometer dimension clusters in silica by the solâ€gel process. Applied Physics Letters, 1996, 68, 3820-3822.	3.3	124
6	Antibacterial coatings on haemodialysis catheters by photochemical deposition of silver nanoparticles. Journal of Materials Science: Materials in Medicine, 2011, 22, 2005-2012.	3.6	100
7	Tuning InAs/GaAs quantum dot properties under Stranski-Krastanov growth mode for 1.3 μm applications. Journal of Applied Physics, 2002, 91, 6710.	2.5	95
8	Annealing behavior of silver, copper, and silver–copper nanoclusters in a silica matrix synthesized by the solâ€gel technique. Journal of Applied Physics, 1996, 80, 6734-6739.	2.5	90
9	Enhanced thermal conductivity in Cu/diamond composites by tailoring the thickness of interfacial TiC layer. Composites Part A: Applied Science and Manufacturing, 2018, 113, 76-82.	7.6	80
10	Synthesis and structural characterisation of CdS nanoparticles prepared in a four-components "water-in-oil―microemulsion. Micron, 2000, 31, 253-258.	2.2	76
11	Tailoring MWCNTs and β-Cyclodextrin for Sensitive Detection of Acetaminophen and Estrogen. ACS Applied Materials & Interfaces, 2018, 10, 21411-21427.	8.0	66
12	Porous Silica-Coated alpha-Fe2O3 Ceramics for Humidity Measurement at Elevated Temperature. Journal of the American Ceramic Society, 1996, 79, 927-937.	3.8	65
13	Biphase TiO ₂ Microspheres with Enhanced Photocatalytic Activity. Industrial & Engineering Chemistry Research, 2014, 53, 7931-7938.	3.7	65
14	Studies of two-dimensional h-BN and MoS2 for potential diffusion barrier application in copper interconnect technology. Npj 2D Materials and Applications, 2017, 1, .	7.9	57
15	Plasma-Deposition of Ag-Containing Polyethyleneoxide-Like Coatings. Plasmas and Polymers, 2000, 5, 1-14.	1.5	54
16	Peroxidase-like properties of Ruthenium nanoframes. Science Bulletin, 2016, 61, 1739-1745.	9.0	45
17	Nonpolar Resistive Switching of Multilayerâ€hBNâ€Based Memories. Advanced Electronic Materials, 2020, 6, 1900979.	5.1	42
18	Structural study of InGaAs/GaAs quantum dots grown by metalorganic chemical vapor deposition for optoelectronic applications at 1.3 μm. Journal of Applied Physics, 2001, 89, 4341-4348.	2.5	41

MASSIMO CATALANO

#	Article	IF	CITATIONS
19	High stability of ultra-small and isolated gold nanoparticles in metal–organic framework materials. Journal of Materials Chemistry A, 2019, 7, 17536-17546.	10.3	41
20	Microstructural characterization of MoO3–TiO2 nanocomposite thin films for gas sensing. Sensors and Actuators B: Chemical, 2001, 77, 27-34.	7.8	40
21	Chemical aspects in copperâ€implanted fused silica and sodaâ€lime glasses. Journal of Applied Physics, 1995, 77, 1294-1300.	2.5	37
22	Enhancing Interconnect Reliability and Performance by Converting Tantalum to 2D Layered Tantalum Sulfide at Low Temperature. Advanced Materials, 2019, 31, e1902397.	21.0	35
23	Enhancement of the optically activated NO2 gas sensing response of brookite TiO2 nanorods/nanoparticles thin films deposited by matrix-assisted pulsed-laser evaporation. Sensors and Actuators B: Chemical, 2012, 161, 869-879.	7.8	34
24	Synthesis and Characterization of Collagen Scaffolds Reinforced by Eggshell Derived Hydroxyapatite for Tissue Engineering. Journal of Nanoscience and Nanotechnology, 2015, 15, 504-509.	0.9	34
25	Indium segregation in N-polar InGaN quantum wells evidenced by energy dispersive X-ray spectroscopy and atom probe tomography. Applied Physics Letters, 2017, 110, .	3.3	34
26	Novel polymeric sorbents based on imprinted Hg(II)-diphenylcarbazone complexes for mercury removal from drinking water. Polymer Journal, 2016, 48, 73-79.	2.7	33
27	Influence of annealing atmosphere on metal and metal alloy nanoclusters produced by ion implantation in silica. Nuclear Instruments & Methods in Physics Research B, 2001, 178, 176-179.	1.4	32
28	Comparison of radiative and structural properties of 1.3 μm InxGa(1â^'x)As quantum-dot laser structures grown by metalorganic chemical vapor deposition and molecular-beam epitaxy: Effect on the lasing properties. Applied Physics Letters, 2003, 82, 3632-3634.	3.3	31
29	Green production of polymer-supported PdNPs: application to the environmentally benign catalyzed synthesis of cis-3-hexen-1-ol under flow conditions. Dalton Transactions, 2012, 41, 12666.	3.3	27
30	Role of oxygen contaminant on the physical properties of sputtered AlN thin films. Journal of Alloys and Compounds, 2015, 649, 1267-1272.	5.5	25
31	(1 0 1) and (0 0 2) oriented AlN thin films deposited by sputtering. Materials Letters, 2017, 200, 18-20.	2.6	24
32	Engineering the Palladium–WSe2 Interface Chemistry for Field Effect Transistors with High-Performance Hole Contacts. ACS Applied Nano Materials, 2019, 2, 75-88.	5.0	24
33	Films of brookite TiO2 nanorods/nanoparticles deposited by matrix-assisted pulsed laser evaporation as NO2 gas-sensing layers. Applied Physics A: Materials Science and Processing, 2011, 104, 963-968.	2.3	23
34	Electrochemical fabrication of nanoporous gold-supported manganese oxide nanowires based on electrodeposition from eutectic urea/choline chloride ionic liquid. Electrochimica Acta, 2013, 87, 918-924.	5.2	23
35	Luminescent Silica-Based Nanostructures from in Vivo Iridium-Doped Diatoms Microalgae. ACS Sustainable Chemistry and Engineering, 2019, 7, 2207-2215.	6.7	23
36	MAPLE deposition of nanomaterials. Applied Surface Science, 2014, 302, 92-98.	6.1	22

MASSIMO CATALANO

#	Article	IF	CITATIONS
37	Atomic Layer Deposition of Layered Boron Nitride for Large-Area 2D Electronics. ACS Applied Materials & Interfaces, 2020, 12, 36688-36694.	8.0	22
38	Structural and electrical characterisation of molybdenum–titanium mixed oxides for ethanol sensing deposited by RF sputtering. Sensors and Actuators B: Chemical, 2003, 92, 286-291.	7.8	20
39	Pulsed laser deposition of a dense and uniform Au nanoparticles layer for surface plasmon enhanced efficiency hybrid solar cells. Journal of Nanoparticle Research, 2013, 15, 1.	1.9	20
40	Controlling Carrier Type and Concentration in NiO Films To Enable <i>in Situ</i> PN Homojunctions. ACS Applied Materials & Interfaces, 2019, 11, 27048-27056.	8.0	20
41	Microphotoluminescence spectroscopy of vertically stackedInxGa1â^'xAs/GaAsquantum wires. Physical Review B, 1998, 58, 1962-1966.	3.2	19
42	Direct quantitative measurement of compositional enrichment and variations in InyGa1â^'yAs quantum dots. Applied Physics Letters, 2001, 79, 3170-3172.	3.3	19
43	Structure and magnetic properties of alloy-based nanoparticles silica composites prepared by ion-implantation and sol–gel techniques. Materials Science and Engineering C, 2001, 15, 59-61.	7.3	18
44	Metal-organic chemical vapor deposition of high quality, high indium composition N-polar InGaN layers for tunnel devices. Journal of Applied Physics, 2017, 121, 185707.	2.5	18
45	The composition and structure of SIPOS: A high spatial resolution electron microscopy study. Journal of Materials Research, 1993, 8, 2893-2901.	2.6	17
46	Noncovalent imprinted microspheres: Preparation, evaluation and selectivity of DBU template. Journal of Applied Polymer Science, 2007, 105, 2190-2197.	2.6	17
47	Quasi-in-Situ Single-Grain Photoelectron Microspectroscopy of Co/PPy Nanocomposites under Oxygen Reduction Reaction. ACS Applied Materials & Interfaces, 2014, 6, 19621-19629.	8.0	17
48	Metal–Organic–Inorganic Nanocomposite Thermal Interface Materials with Ultralow Thermal Resistances. ACS Applied Materials & Interfaces, 2017, 9, 10120-10127.	8.0	17
49	Metal-organic chemical vapor deposition of N-polar InN quantum dots and thin films on vicinal GaN. Journal of Applied Physics, 2018, 123, .	2.5	17
50	Growth assessment of (002)-oriented AlN thin films on Ti bottom electrode deposited on silicon and kapton substrates. Materials and Design, 2017, 119, 151-158.	7.0	16
51	Structural and optical properties of molybdenum–tungsten mixed oxide thin films deposited by the sol-gel technique. Journal of Applied Physics, 2003, 93, 3816-3822.	2.5	15
52	Dependence of h-BN Film Thickness as Grown on Nickel Single-Crystal Substrates of Different Orientations. ACS Applied Materials & Interfaces, 2018, 10, 44862-44870.	8.0	15
53	A modeling and convolution method to measure compositional variations in strained alloy quantum dots. Ultramicroscopy, 2003, 94, 1-18.	1.9	14
54	Au nanoparticles decoration of silica nanowires for improved optical bio-sensing. Sensors and Actuators B: Chemical, 2016, 226, 589-597.	7.8	14

MASSIMO CATALANO

#	Article	IF	CITATIONS
55	High-κ Dielectric on ReS2: In-Situ Thermal Versus Plasma-Enhanced Atomic Layer Deposition of Al2O3. Materials, 2019, 12, 1056.	2.9	14
56	Critical issues in the focused ion beam patterning of nanometric hole matrixes on GaAs based semiconducting devices. Nanotechnology, 2006, 17, 1758-1762.	2.6	13
57	Electrical and optical properties of ITO and ITO/Cr-doped ITO films. Applied Physics A: Materials Science and Processing, 2010, 101, 753-758.	2.3	13
58	Structural and morphological evolution of aluminum nitride thin films: Influence of additional energy to the sputtering process. Journal of Physics and Chemistry of Solids, 2013, 74, 1444-1451.	4.0	13
59	Engineering the interface chemistry for scandium electron contacts in WSe ₂ transistors and diodes. 2D Materials, 2019, 6, 045020.	4.4	13
60	Structural characterization of lattice matched AlxIn1â^'xAs/InP and GayIn1â^'yAs/InP heterostructures by transmission electron microscopy and highâ€resolution xâ€ray diffraction. Journal of Applied Physics, 1995, 78, 2403-2410.	2.5	12
61	Influence of different V-grooved GaAs substrates on the geometrical shape of InGaAs/GaAs quantum wires. Journal of Crystal Growth, 1999, 197, 777-782.	1.5	12
62	Preparation and characterisation of organic–inorganic heterojunction based on BDA-PPV/CdS nanocrystals. Materials Science and Engineering B: Solid-State Materials for Advanced Technology, 2000, 74, 175-179.	3.5	12
63	Direct bonding of copper and liquid crystal polymer. Materials Letters, 2018, 212, 214-217.	2.6	11
64	Structural characterization of ultrathin Cr-doped ITO layers deposited by double-target pulsed laser ablation. Journal Physics D: Applied Physics, 2011, 44, 365403.	2.8	10
65	Nanoscale compositional fluctuations in multiple InGaAs/GaAs quantum wires. Journal of Applied Physics, 2000, 87, 2261-2264.	2.5	9
66	Nanoscale Compositional Fluctuations in Single InGaAs/GaAs Quantum Dots. Physica Status Solidi (B): Basic Research, 2001, 224, 17-20.	1.5	8
67	Inter-level carrier dynamics and photocurrent generation in large band gap quantum dot solar cell by multistep growth. Solar Energy Materials and Solar Cells, 2017, 171, 142-147.	6.2	8
68	Structure and chemistry of Ag‒Cu nanoclusters in a silica matrix by the sol-gel process. The Philosophical Magazine: Physics of Condensed Matter B, Statistical Mechanics, Electronic, Optical and Magnetic Properties, 1997, 76, 621-628.	0.6	7
69	Electronic structure of double stacked InAsâ^•GaAs quantum dots: Experiment and theory. Journal of Applied Physics, 2007, 102, 094314.	2.5	7
70	Optical Absorption Measurements at High Temperature (500 °C) of Oxide Nanoparticles for Application as Gas-Based Nanofluid in Solar Thermal Collector Systems. Advanced Materials Research, 0, 773, 80-86.	0.3	7
71	Block Copolymer and Cellulose Templated Mesoporous TiO2-SiO2 Nanocomposite as Superior Photocatalyst. Catalysts, 2022, 12, 770.	3.5	7
72	Correlation between shape and electronic states in nanostructures. Micron, 2000, 31, 245-251.	2.2	6

#	Article	IF	CITATIONS
73	Optimization of electron beam induced deposition process for the fabrication of diode-like Pt/SiO2/W devices. Journal of Vacuum Science and Technology B:Nanotechnology and Microelectronics, 2013, 31, 041805.	1.2	5
74	Dy- and Tb-doped CeO2-Ni cermets for solid oxide fuel cell anodes: electrochemical fabrication, structural characterization, and electrocatalytic performance. Journal of Solid State Electrochemistry, 2018, 22, 3761-3773.	2.5	5
75	The effects of the focus ion beam milling process on the optical properties of semiconductor nanostructures. Nanotechnology, 2009, 20, 255306.	2.6	4
76	Morphological and compositional effects of FIB nanopatterning of multilayer metal/semiconducting devices. Physica E: Low-Dimensional Systems and Nanostructures, 2009, 41, 734-738.	2.7	4
77	Substrate-Au catalyst influence on the growth of ZnO nanorods. Materials Science and Engineering B: Solid-State Materials for Advanced Technology, 2010, 172, 225-230.	3.5	4
78	Study of titania nanorod films deposited by matrix-assisted pulsed laser evaporation as a function of laser fluence. Applied Physics A: Materials Science and Processing, 2011, 105, 605-610.	2.3	4
79	Microstructural and Microanalytical Characterization of Pd Clusters in ORMOCER Matrix. Microscopy Microanalysis Microstructures, 1995, 6, 611-619.	0.4	4
80	Metal Nanocrystals in Amorphous Silica Matrix by the Sol-Gel Process. Materials Science Forum, 1996, 203, 59-64.	0.3	3
81	Time resolved screening of the piezoelectric field in InGaAs/GaAs V-shaped quantum wires of variable profile. Journal of Physics Condensed Matter, 1999, 11, 5989-5997.	1.8	3
82	Effects of coupling on the structural properties of InxGa1â^'xAs/GaAs 1-D and 0-D self-organized quantum structures. Materials Science and Engineering B: Solid-State Materials for Advanced Technology, 2001, 87, 256-261.	3.5	3
83	Molybdenum-based nanostructured mixed oxides for sensing applications: Effect of the Mo oxide composition on the structure of sol–gel thin films. Journal of Vacuum Science & Technology an Official Journal of the American Vacuum Society B, Microelectronics Processing and Phenomena, 2002, 20, 2433.	1.6	3
84	Structural, Morphological, and Chemical Properties of Cu/TiN Versus Cu Thin Layers for HEMT Backside Metallization. IEEE Transactions on Device and Materials Reliability, 2014, 14, 890-897.	2.0	3
85	Morphological and structural characterization of Sm–O–S compounds prepared by thermolysis of dithiocarbamate precursors. Thin Solid Films, 2014, 556, 241-246.	1.8	3
86	Physical insight in the fluence-dependent distributions of Au nanoparticles produced by sub-picosecond UV pulsed laser ablation of a solid target in vacuum environment. Applied Surface Science, 2019, 480, 330-340.	6.1	3
87	Recombination in InGaAs/GaAs quantum wire lasers. Solid State Communications, 1999, 112, 55-60.	1.9	2
88	Effects of quantum mechanical coupling on the optical properties of vertically stacked V-groove quantum wires. Journal of Applied Physics, 2000, 88, 772-776.	2.5	2
89	Optimization of Digital Growth of Thick N-Polar InGaN by MOCVD. Journal of Electronic Materials, 2020, 49, 3450-3454.	2.2	2
90	TEM Characterization of Palladium and Silver Nanoclusters in Glass Matrix. Materials Science Forum, 1995, 195, 87-92.	0.3	1

#	Article	IF	CITATIONS
91	TEM characterization of single and multiple InGaAs/GaAs quantum wires grown by metal–organic vapor phase epitaxy on V-grooved substrates. Materials Science and Engineering B: Solid-State Materials for Advanced Technology, 1999, 67, 39-45.	3.5	1
92	Fabrication and characterization of strained InGaAs quantum wires grown on high index V-grooved GaAs substrates by LP-MOVPE. Superlattices and Microstructures, 1999, 25, 481-485.	3.1	1
93	Time-resolved magneto-optical properties of V-shaped single quantum wires. Physica E: Low-Dimensional Systems and Nanostructures, 2000, 7, 536-540.	2.7	1
94	Influence of the N2/H2 ratio on the structural features of InxGa1â^'xN/GaN films grown by MOCVD. Materials Science and Engineering B: Solid-State Materials for Advanced Technology, 2001, 87, 237-243.	3.5	1
95	Luminescence Following Highly Localized Hole Carrier Injection into InGaAs Quantum Dots. Japanese Journal of Applied Physics, 2002, 41, 5127-5128.	1.5	1
96	High Spatial Resolution Energy Dispersive X-ray Spectroscopy and Atom Probe Tomography study of Indium segregation in N-polar InGaN Quantum Wells. Microscopy and Microanalysis, 2017, 23, 1448-1449.	0.4	1
97	InAs/AlGaAs quantum dots grown by a novel molecular beam epitaxy multistep design for intermediate band solar cells: physical insight into the structure, composition, strain and optical properties. CrystEngComm, 2019, 21, 4644-4652.	2.6	1
98	Scanning transmission electron microscopy determination of critical InAs QD parameters from high-quality focused ion beam lamellas. Semiconductor Science and Technology, 2009, 24, 085001.	2.0	0
99	Edge-melting: nanoscale key-mechanism to explain nanoparticle formation from heated TEM grids. Applied Surface Science, 2016, 365, 191-201.	6.1	0